Mechanistic insight into the impact of a bivalent ligand on the structure and dynamics of a GPCR oligomer

Samman Mansoor,[†] Gülru Kayık,[‡] Serdar Durdagi,[‡] and Ozge Sensoy[*,¶,§]

[†]*School of Engineering and Natural Sciences, Department of Biomedical Engineering and Bioinformatics, Istanbul Medipol University, Turkey*

[‡]*Computational Biology and Molecular Simulations Laboratory, Department of Biophysics, School of Medicine, Bahcesehir University, Istanbul, Turkey*

[¶]*Regenerative and Restorative Medicine Research Center (REMER), Research Institute for Health Sciences and Technologies (SABITA), Istanbul Medipol University, 34810, Istanbul, Turkey*

[§]*School of Engineering and Natural Sciences, Department of Computer Engineering , Istanbul Medipol University, Turkey*

E-mail: osensoy@medipol.edu.tr

Reweighting

Given the boost potential of each frame the probability of reaction coordinates can be reweighted to recover the canonical ensemble distribution of the system. To reduce the noise generated by huge data points the cumulant expansion approximation is better considered to calculate the ensemble-averaged reweighting, the cumulant expansion can be obtained by the given equation;

$$(e^{\beta\Delta V}) = exp\Big\{\sum_{k=1}^{\infty}\frac{\beta^k}{k!}C_k\Big\} \tag{1}$$

$(e^{\beta\Delta V})$ ensemble-averaged reweighting factor, C_2 is the cumulant expansion to the second order where $(\sigma^2_{\Delta V})$ in equation 2 represents the standard deviation of boost potential ΔV;

$$C_2 = \langle\Delta V^2\rangle - \langle\Delta V\rangle^2 = \sigma^2_{\Delta V} \tag{2}$$

The free energy can then be derived from cumulant expansion as:

$$F(A_j) = F^*(A_j) - \frac{1}{\beta}\sum_{k=1}^{\infty}\frac{\beta^k}{k!}C_k + F_c \tag{3}$$

where $F^*(A^j)$ is the modified free energy surface sampled in the aMD simulation and the constant $F_c = (1/\beta)ln\sum_{j=1}^{M}\langle e^{\beta\Delta V(r)}\rangle_j$ where M is the number of bins and $\beta = 1/k_BT$ for simulation found in j^{th} bin. The PMF (potential mean force) has been calculated for χ_2 Trp246$^{6.48}$ has been shown in Figure 1. We also observed an overlap between energy minima pertaining to volume changes (Figure 3) and χ_2 of Trp246$^{6.48}$ (Figure 5A) obtained in cMD and aMD simulations. Here, it is important to emphasize that the ionic lock distance (Figure 7C) did not sample higher values in cMD in the without linker system as opposed to aMD yet the energy minima were still overlapped.

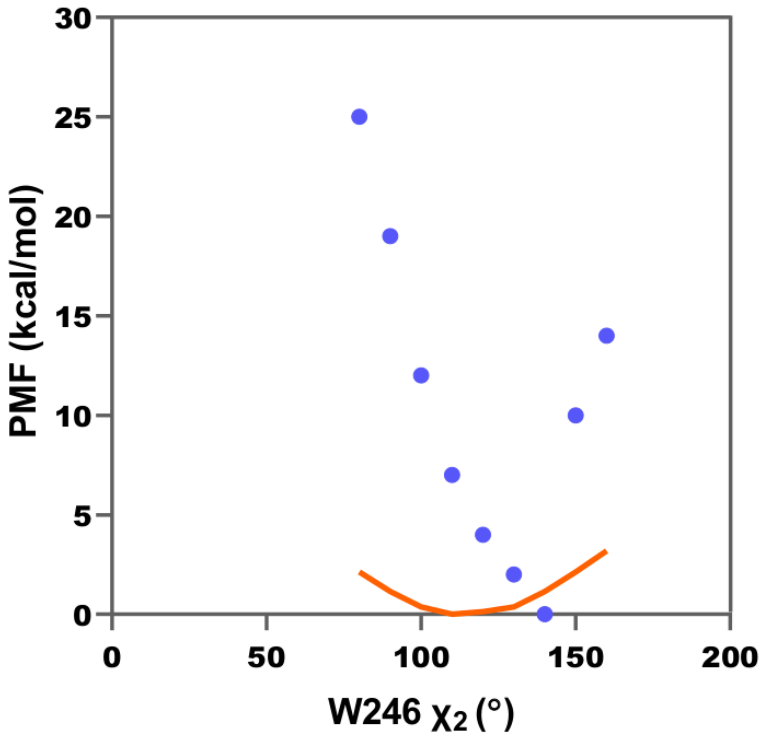

Figure 1: PMF profiles of the χ_2 Trp246$^{6.48}$ obtained from reweighting based on cumulant expansion to the 2nd order (blue) and calculated from classical MD simulation (orange) for comparison.[1,2]

Having seen the large noise in reweighted profiles we checked if unweighted data can be used to discuss changes by comparing unweighted PMF profiles to those obtained from cMD. Herein, it is important to point out that cMD simulations might not be relevant for the comparison since these simulations were short and performed to get average dihedral and potential energy values required for aMD simulations. So, it is likely that some energy minima might not have been sampled. We started comparison with χ_2 angle of Tyr288$^{7.53}$ of antagonist-bound $A_{2A}R$ (Figure 5B) as it displayed two peaks, thus presenting a challenging reaction coordinate. Interestingly, the two minima sampled in cMD and aMD simulations were similar in spite of energy difference between them-being higher in cMD as shown below in Figure 2. This is -in fact- in correspondence with the theory of aMD which states that the barrier that separates energy minima is decreased in aMD simulations. However, it is still true that although the shape of the energy profile is conserved the probabilities of these

regions of energy minima might be different. For our purposes, the values of energy minima are more important as they correspond to most possible conformations of the target residues as indicated in the manuscript. Also, the minima are different between without linker and linker systems which make it possible to compare them on the plots. Considering that the barriers that separate energy minima decrease while the overall shape of the energy profiles is conserved in aMD simulations, unweighted data can be considered as an estimate of the original free energy profile.

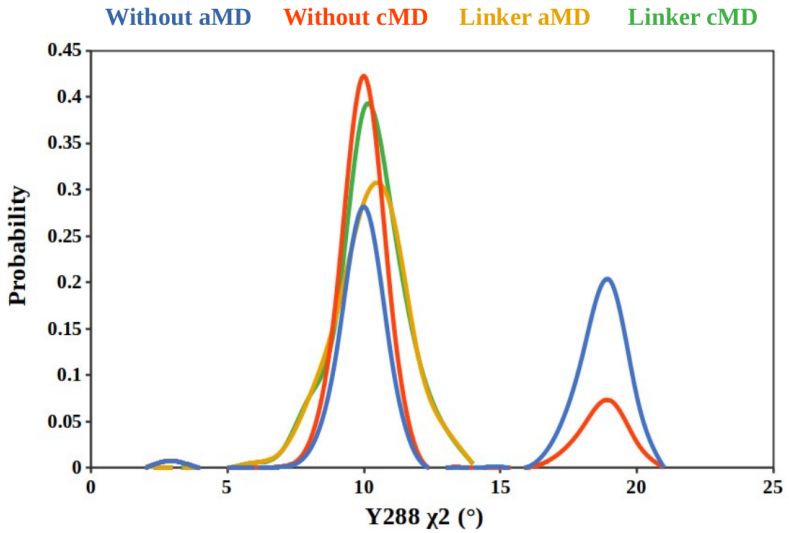

Figure 2: Comparison of probability distributions pertaining χ_2 Tyr288$^{7.53}$ obtained in aMD without linker, cMD without linker, aMD linker and cMD linker which are shown in blue, red, yellow and green, respectively.

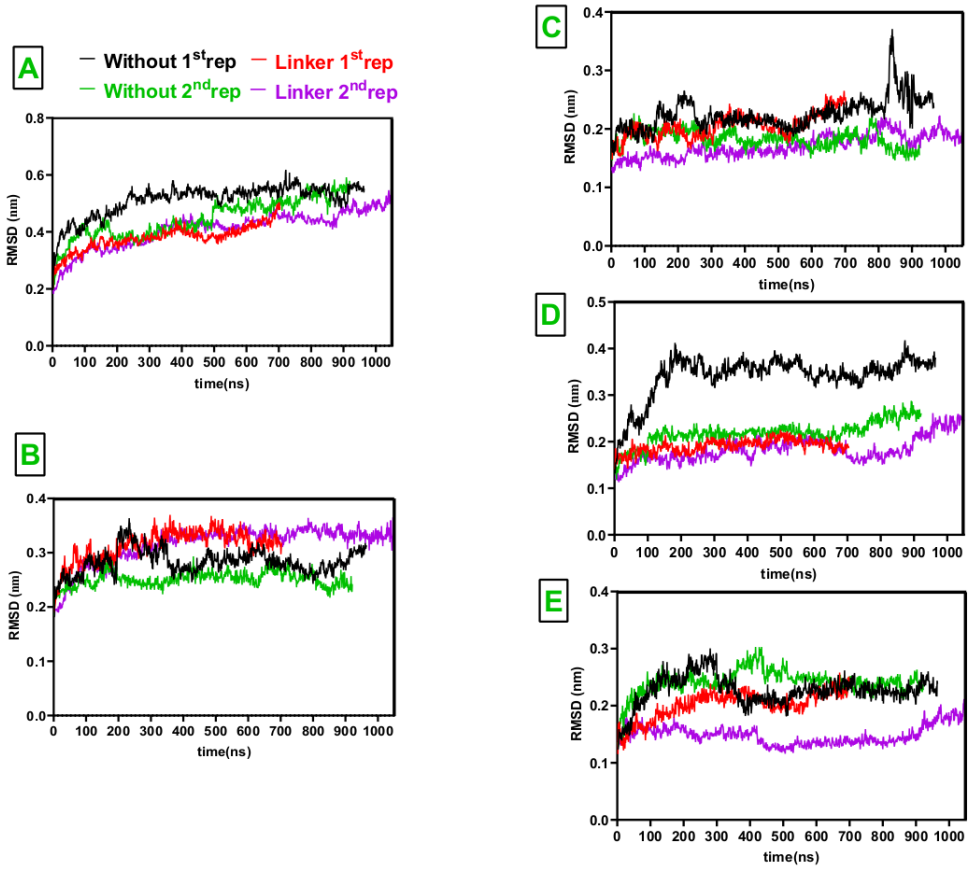

Figure 3: **Root Mean Square Deviation (RMSD) timeline plots. A.** Tetramer. **B.** Agonist bound D_2R. **C.** Apo D_2R. **D.** Antagonist bound $A_{2A}R$. **E.** Agonist bound $A_{2A}R$.

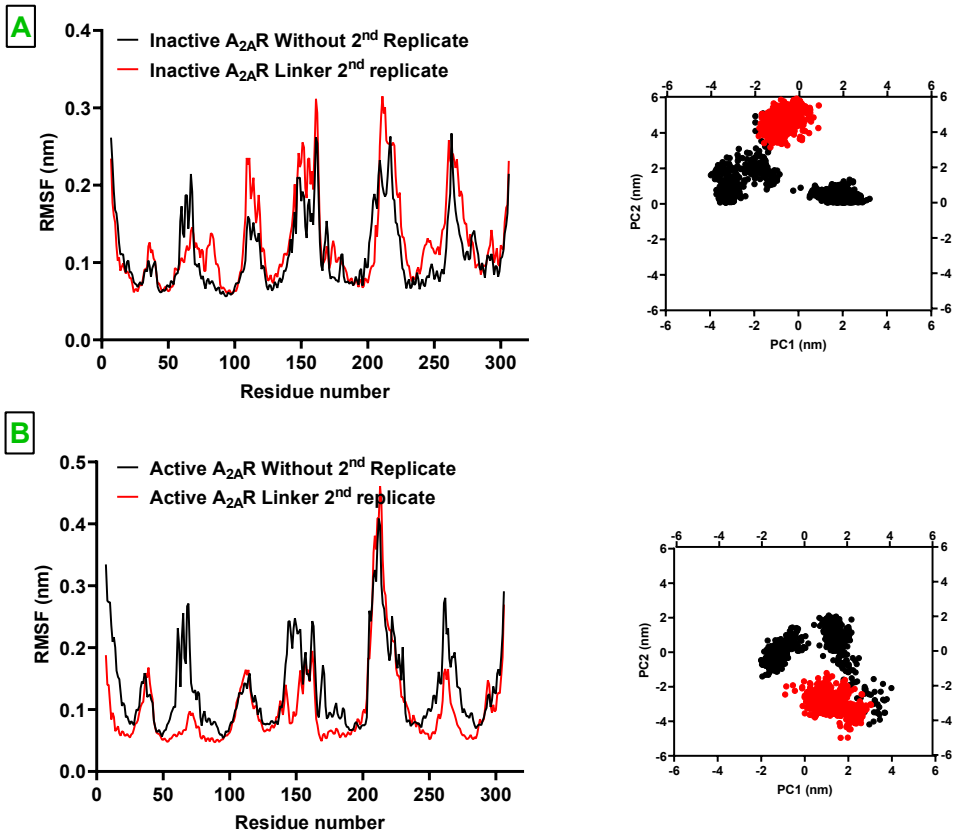

Figure 4: **RMSF and 2D-PCA plots of second replicate of $A_{2A}R$ dimer. A**. represent inactive $A_{2A}R$ along its PCA plot **B**. represents active $A_{2A}R$ along its PCA plot.

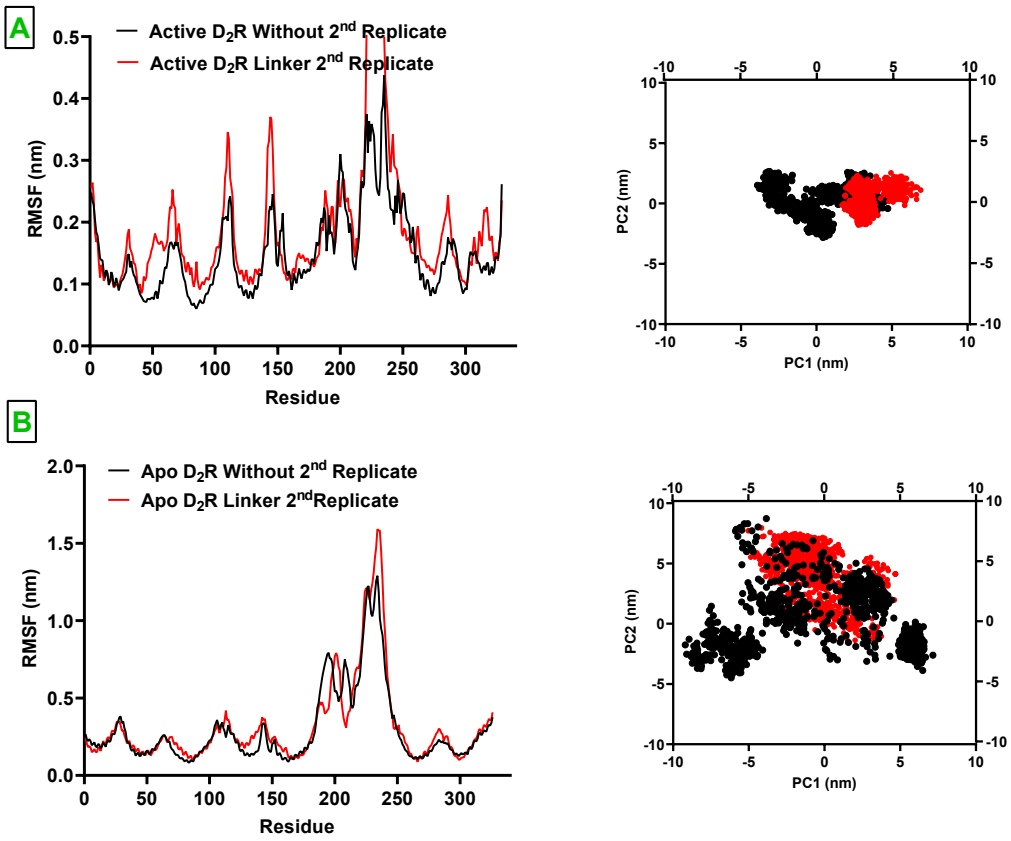

Figure 5: **RMSF and 2D-PCA plots of second replicate of D_2R dimer A**. represent active D_2R along its PCA plot **B**. represents *apo* D_2R along its PCA plot.

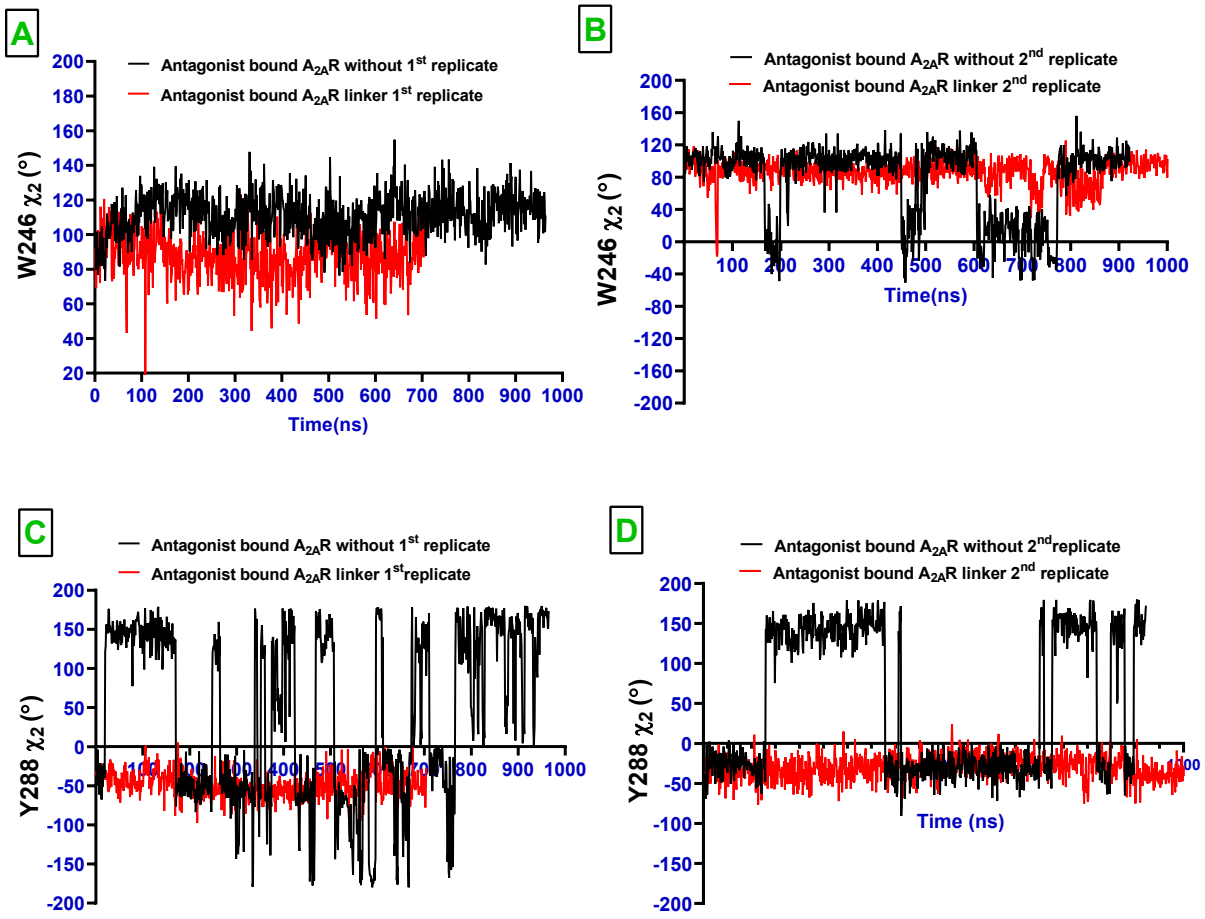

Figure 6: **Timeline plots of both replicates of $A_{2A}R$ microswitches Trp246$^{6.48}$ and Tyr288$^{7.53}$.** **(A and B)** χ_2 angle probability of both replicates of Toggle switch Trp246$^{6.48}$ inactive $A_{2A}R$. **(C and D)** χ_2 angle probability of both replicates of Tyrosine Rotamer Tyr288$^{7.53}$ inactive $A_{2A}R$.

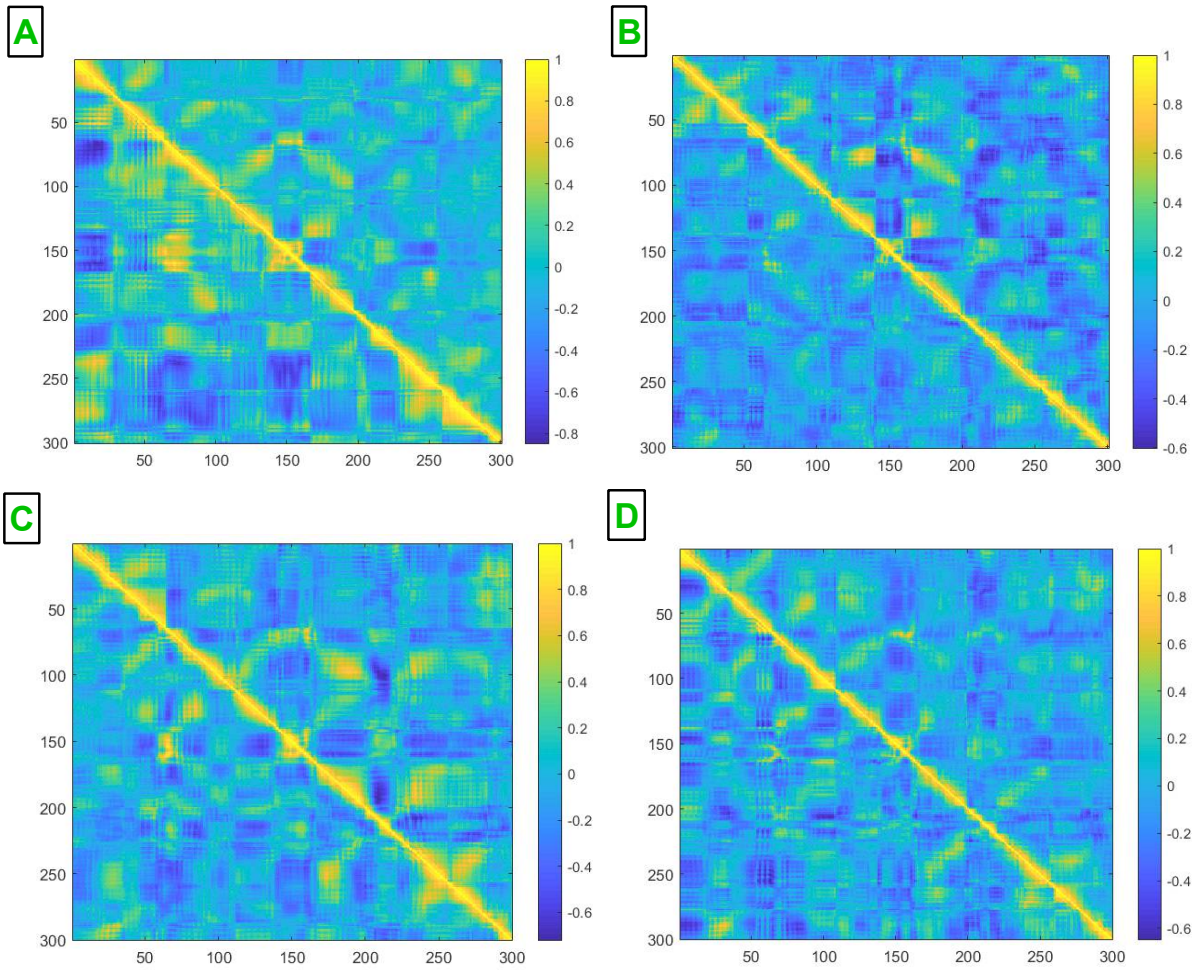

Figure 7: **DCCM Plots of all replicates of $A_{2A}R$** In all the plots linker systems are represented above the diagonal and without linker system shown below the diagonal line. **A.** represent 1st replicate of inactive $A_{2A}R$ **B.** represents 2nd replicate of inactive $A_{2A}R$ **C.** represents 1st replicate of active $A_{2A}R$ **D.** represents 2nd replicate of active $A_{2A}R$

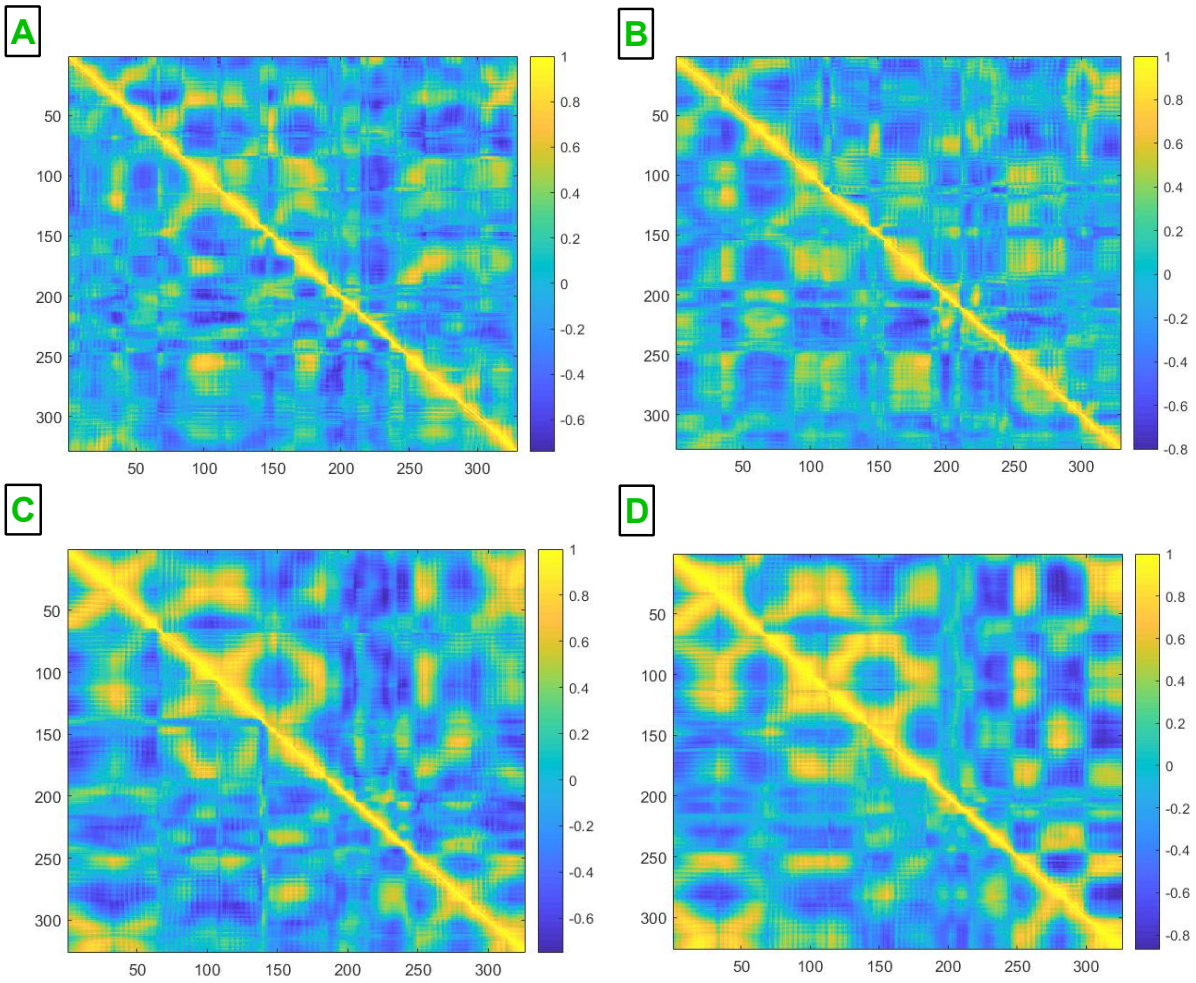

Figure 8: **DCCM Plots of all replicates of D_2R.** In all the plots linker systems are represented above the diagonal and without linker system shown below the diagonal line. **A.** represent 1st replicate of active D_2R **B**. represents 2nd replicate of active D_2R **C.** represents 1st replicate of apo D_2R **D.** represents 2nd replicate of apo D_2R

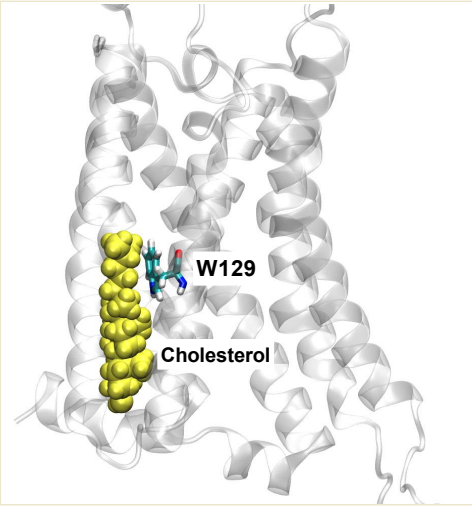

Figure 9: **Cholesterol binding residue shown for Agonist bound $\mathbf{A_{2A}R}$**. Cholesterol molecule is shown in van der Waals representation in yellow color and Trp129$^{4.50}$ in licorice representation, keeps their interaction during the course of simulation in one of the replicate of agonist bound $A_{2A}R$

Table 1: Templates used to model the interfaces in the tetramer

Receptor	PDB IDs	Interface
$A_{A2}R$	5IU4	TM4-5
$A_{A2}R$	5IU7	TM4-5
$A_{A2}R$	5IU8	TM4-5
$A_{A2}R$	5IUA	TM4-5
$A_{A2}R$	5IUB	TM4-5
$A_{A2}R$	5JTB	TM4-5
$A_{A2}R$	5K2A	TM4-5
$A_{A2}R$	5K2B	TM4-5
$A_{A2}R$	5K2C	TM4-5
$A_{A2}R$	5K2D	TM4-5
$A_{A2}R$	5MZJ	TM4-5
$A_{A2}R$	5MZP	TM4-5
$A_{A2}R$	5N2R	TM4-5
$A_{A2}R$	5NLX	TM4-5
$A_{A2}R$	5NM2	TM4-5
$A_{A2}R$	5NM4	TM4-5
$A_{A2}R$	5OLG	TM4-5
$A_{A2}R$	5OLH	TM4-5
$A_{A2}R$	5OLO	TM4-5
$A_{A2}R$	5OLV	TM4-5
$A_{A2}R$	5OLZ	TM4-5
$A_{A2}R$	5OM1	TM4-5
$A_{A2}R$	5OM4	TM4-5
$A_{A2}R$	5UVI	TM4-5
$A_{A2}R$	5VRA	TM4-5
$A_{A2}R$	6AQF	TM4-5
$A_{A2}R$	4EIY	TM4-5
ADRB1	4GPO	TM4-5
ADRB1	5F8U	TM4-5
ADRB2	3D4S	TM4-5
C5AR1	5O9H	TM4-5
OPSD	2Z73	TM4-5
OPSD	3AYM	TM4-5
OPSD	3AYN	TM4-5
OPSD	4WW3	TM4-5
P2Y12	4NTJ	TM4-5
SMO	4JKV	TM4-5
SMO	4QIN	TM4-5
D4R	5WIU	TM6-6
D4R	5WIV	TM6-6

References

(1) Miao, Y.; Nichols, S. E.; McCammon, J. A. Free energy landscape of G-protein coupled receptors, explored by accelerated molecular dynamics. *Physical Chemistry Chemical Physics* **2014**, *16*, 6398–6406.

(2) Zhang, F.; Yuan, Y.; Li, H.; Shen, L.; Guo, Y.; Wen, Z.; Pu, X. Using accelerated molecular dynamics simulation to shed light on the mechanism of activation/deactivation upon mutations for CCR5. *RSC advances* **2018**, *8*, 37855–37865.